Joint Optimization of Precoder and Equalizer in MIMO VLC Systems

Kai Ying, *Student Member, IEEE*, Hua Qian, *Senior Member, IEEE*, Robert J. Baxley, *Senior Member, IEEE*, and Saijie Yao

***Abstract*—Recently, visible light communication (VLC) has attracted much attention as a possible candidate technology to meet the ever growing demand in wireless data. However, current low-cost white LED has limited modulation bandwidth, which limits the throughput of the VLC. Optical MIMO can provide spatial diversity and thus achieve high data rate. Traditional multiple-input multiple-output (MIMO) techniques used in wireless communications cannot be directly applied to VLC. This paper studies the precoder and equalizer design of optical wireless MIMO system for VLC. First, we propose a MIMO VLC system, which can effectively support the flickering/dimming control and other VLC-specific requirements. Second, besides the transceiver design with perfect channel state information, we also take into account channel uncertainties for joint optimization in the MIMO VLC system. Numerical results show that the proposed MIMO solution for VLC is robust to combat the influence caused by the channel estimation imperfection. By taking into account the channel estimation errors, the proposed joint optimization method demonstrates the bit error rate (BER) improvements in the scenario of imperfect channel estimation.**

***Index Terms*—Visible light communication, optical MIMO, transceiver design, channel uncertainty, brightness control.**

I. Introduction

In recent years, visible light communication (VLC) has attracted significant interests in both academic and industrial worlds due to the massive deployment of lighting emitting diodes (LEDs) [1]. Moreover, VLC serves as a possible candidate to address the current challenges in wireless communications such as the bandwidth limitation, the electromagnetic radiation, and the energy efficiency. VLC has been standardized for wireless personal area networks (WPANs) in IEEE 802.15.7 [2] and is on the way to commercialization.

Manuscript received May 28, 2014; revised November 10, 2014; accepted April 24, 2015. Date of publication May 13, 2015; date of current version August 17, 2015. This work was supported in part by the 100 Talents Program of Chinese Academy of Sciences, the National Key Science and Technology Project (No. 2014ZX03003012), the Science and Technology Commission Foundation of Shanghai (No. 13511507502), and the National Science Foundation (No. ECCS-1343256).

K. Ying is with the School of Electrical and Computer Engineering, Georgia Institute of Technology, Atlanta, GA 30332 USA (e-mail: kying3@gatech.edu).

H. Qian and S. Yao are with the Key Laboratory of Wireless Sensor Network and Communication, Shanghai Research Center for Wireless Communications, Shanghai Institute of Microsystem and Information Technology, CAS, Shanghai 200335, China (e-mail: hua.qian@wico.sh; saijie.yao@wico.sh).

R. J. Baxley is with Bastille Networks, Atlanta, GA 30318 USA (e-mail: bob.baxley@gmail.com).

Color versions of one or more of the figures in this paper are available online at http://ieeexplore.ieee.org.

Digital Object Identifier 10.1109/JSAC.2015.2432515

On the other hand, the low-cost white LED has limited modulation bandwidth, which prohibits high transmission rate of VLC. Optical multiple-input multiple-output (MIMO) can help to achieve high data rate by utilizing spatial diversity [3]. However, different from radio frequency (RF) systems, optical front end always employs simple intensity modulation and direct detection (IM/DD) techniques. The decorrelation from different spatial data streams becomes the bottleneck [4]. Some methods such as power imbalance, cross links blocking or artificial neural network can help overcome this problem [5]–[7]. Moreover, imaging receivers have been widely accepted to reduce the MIMO channel correlation and utilize the spatial multiplexing [4], [8], [9]. In addition, orthogonal frequency division multiplexing (OFDM) can be also deployed together with MIMO in VLC systems to further enhance the bandwidth utilization efficiency and boost the data rates [10], [11]. Some experimental results have demonstrated that high data rates up to gigabit/s can be achieved in the MIMO VLC system [11].

In the area of MIMO VLC system, the precoder and equalizer design is still open to researchers. In previous works, a simple way to design the transceiver in MIMO VLC systems was to apply the channel matrix inversion at the receiver side [4], [7], [8], [11]. If the channel matrix was rank-deficient or not squared, pseudo-inversion operation was used instead. However, these methods might result in noise amplification if the values of elements in the channel matrix were low [13], [14]. An optimal transceiver design is desired. MIMO schemes based on the singular value decomposition (SVD) architecture are commonly used in RF systems to obtain parallel channels. These traditional techniques cannot be directly applied to MIMO VLC systems, since lighting requirements such as dimming/brightness control and nonnegativity of the intensity modulation are always challenges in the transceiver design [2]. In [5], power and offset allocation with adaptive modulation was well discussed in SVD-based MIMO systems for optical wireless channels, but dimming control was not supported. Authors in [12] proposed a modified SVD-VLC MIMO system to meet the illumination constraints, but additional adjusting should be applied to the input signals so that both the nonnegativity of the intensity modulation and dimming control can be satisfied. In this paper, we propose a MIMO VLC system, which can effectively support the flickering/dimming control and other lighting requirements. Moreover, in such a system, the precoder and equalizer can be adaptively optimized according to different input signals and various illumination levels.

Moreover, in many studies, the optical MIMO channel matrix was assumed to be perfectly known [4]–[14]. However, the

perfect estimation is not always available due to the time-varying nature of wireless optical channels and limited length of training. In [5], [7], [13], authors pointed out that channel estimation errors would result in system performance degradation severely. A second contribution of this paper is that we take into account channel uncertainties in joint optimization of the MIMO VLC system. Both a non-robust minimum mean-square error (MMSE) scheme and a robust MMSE scheme are proposed. Here, the non-robust scheme means that the transceiver design is based on the assumption that channel state information (CSI) is perfectly known. In the robust scheme, the channel estimation errors are taken into account in the joint optimization of the procoder and equalizer. By taking into account the channel estimation errors, the proposed joint optimization method can improve the performance in the scenario of imperfect channel estimation.

The rest of the paper is organized as follows. Section II discusses about MIMO channels for VLC system. The proposed MIMO VLC system is described in Section III. In Section IV we study the joint precoder and equalizer design with perfect channel information. Then, we discuss the joint design with imperfect channel information in Section V. Numerical results are presented in Section VI. Finally, Section VII concludes the paper.

Notation: To simplify discussions in the rest of this paper, we summarize the mathematical notations here. In this paper, uppercase and lowercase letters denote matrices and vectors, respectively; operator $(\cdot)^T$, $(\cdot)^H$, $(\cdot)^{-1}$ denote the transpose, conjugate transpose and inverse of a matrix/vector, respectively; $(\cdot)^{\frac{1}{2}}$ denotes square root of a square matrix; $\mathbf{I}_N$ is an $N \times N$ identity matrix; $\mathbb{E}_{\mathbf{X}}\{\cdot\}$ denotes the statistical expectation over $\mathbf{X}$; $Tr(\cdot)$ is the trace of a matrix; $Re\{\cdot\}$ denotes the real part of a variable; vec$(\cdot)$ represents the matrix vectorization; $\otimes$ denotes the Kronecker product; $\|\cdot\|$ denotes the Frobenius norm; and abs$(\cdot)$ denotes an element-wise absolute operator.

II. MIMO Channel in VLC System

In the VLC system, there are two types of links. One is the direct point-to-point line-of-sight (LOS) link and the other is the diffuse link caused by reflections. In most cases, only the LOS link is considered since it is usually much stronger than the diffuse link [3], [4], [6]–[13]. Authors in [4] showed that even the strongest multipath component was at least 7 dB lower than the weakest LOS component. In [13], it was pointed out that no multipath interference would occur at data rates below several hundreds Mb/s according to a root mean square delay spread investigation. Practically, the emission from an LED can be modeled by a generalized Lambertian radiant intensity [15]:

$$R_o(\phi) = \frac{m+1}{2\pi}\cos^m\phi \tag{1}$$

where ϕ is the angle of emission relative to the optical axis of the emitter; m is the order of Lambertian emission given by $m = -\ln 2/\ln(\cos\Phi_{\frac{1}{2}})$ and $\Phi_{\frac{1}{2}}$ is the transmitter semiangle (at half power).

At the receiver, the photodetector (PD), the frequency response of LOS channel is relatively flat near DC, which can be modeled as

$$h = \begin{cases} \frac{A}{d^2}R_o(\phi)\cos\theta, & \text{for } \theta \le \Theta_{\frac{1}{2}}, \\ 0, & \text{for } \theta > \Theta_{\frac{1}{2}} \end{cases} \tag{2}$$

where θ is the angle of incidence with respect to the receiver axis; $\Theta_{\frac{1}{2}}$ is the field-of-view (FOV) semiangle of receiver; A is the detector area of receiver; and d is the distance between the transmitter and the receiver [16].

Considering the channel for a MIMO VLC system, where signals are transmitted by multiple LEDs and received by multiple PDs, the MIMO channel matrix H can be determined by the direct current (DC) gains among each LED and PD pair [4]:

$$\mathbf{H} = \begin{bmatrix} h_{11} & h_{12} & \cdots & h_{1N_t} \\ h_{21} & h_{22} & \cdots & h_{2N_t} \\ \vdots & \vdots & \ddots & \vdots \\ h_{N_r1} & h_{N_r2} & \cdots & h_{N_rN_t} \end{bmatrix}, \tag{3}$$

where N_t is the number of LEDs and N_r is the number of PDs; and element h_{mn} can be derived from (2) corresponding to the nth LED and the mth PD.

However, channel correlation is a major concern for VLC MIMO. Thus, it is not practical to apply MIMO in VLC system directly since the channel correlation is sensitive to transmitter spacing and receiver position. Intuitively, ill-conditioned channel matrix may occur due to the homogenous behaviors in different channel DC gains [4].

When we discuss VLC MIMO, the channel matrix is deterministic if the positions of LEDs and PDs are fixed. The channel correlation implies that the channel matrix is not full-rank or the condition number is very large. The condition number is defined by the ratio of the largest singular value of the channel matrix to the smallest [25].

Fig. 1 shows an example of the MIMO VLC system. Suppose we have a room with size $4m \times 4m \times 4m$. Four LEDs are located at (1, 1, 4), (−1, 1, 4), (−1, −1, 4) and (1, −1, 4) respectively. We assume that the transmitter semiangle $\Phi_{\frac{1}{2}} = 60^\circ$ and thus the order of Lambertian emission $m = 1$. Four PDs are positioned at (0.05, 0.05, 1), (−0.05, 0.05, 1), (−0.05, −0.05, 1) and (0.05, −0.05, 1) and the detector area of each PD is 1 cm^2. The FOV semiangle is assumed to be 30°. Then we have the channel matrix

$$\mathbf{H} = 10^{-5} \times \begin{bmatrix} 0.2454 & 0.2365 & 0.2282 & 0.2365 \\ 0.2365 & 0.2454 & 0.2365 & 0.2282 \\ 0.2282 & 0.2365 & 0.2454 & 0.2365 \\ 0.2365 & 0.2282 & 0.2365 & 0.2454 \end{bmatrix}. \tag{4}$$

By singular value decomposition (SVD), we can obtain a vector of singular values

$$\mathbf{sv} = 10^{-5} \times [0.9466 \quad 0.0172 \quad 0.0172 \quad 0.005]. \tag{5}$$

We observe that the condition number is very large. Thus, the MIMO channel matrix is ill-conditioned. Since the first singular

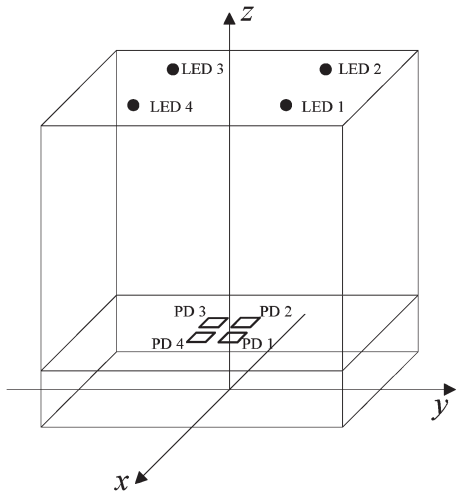

Fig. 1. A scenario of VLC MIMO system deployment.

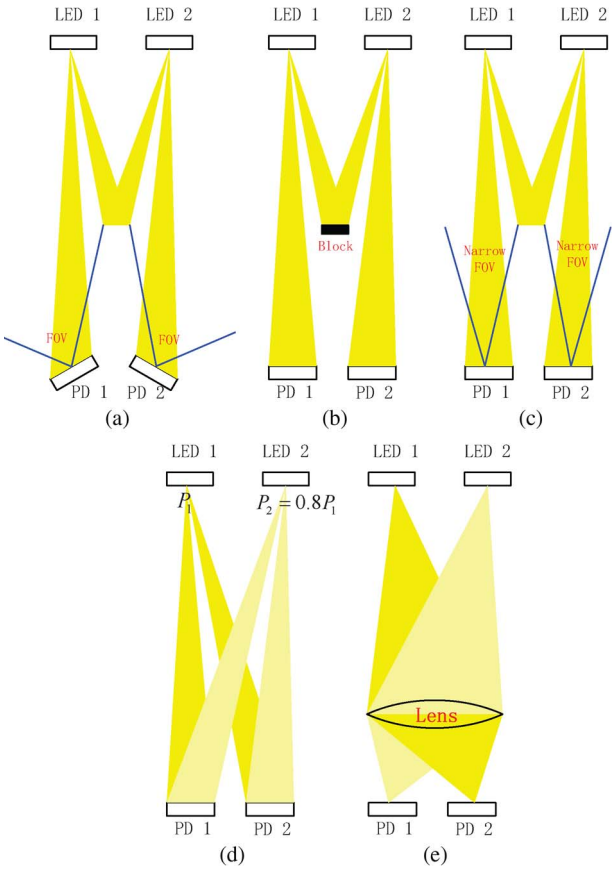

Fig. 2. Methods to reduce channel correlation. (a) Angle adjustment. (b) Blocking. (c) Narrow FOV. (d) Power imbalance. (e) Imaging receiver.

value is much larger than other three, we may obtain only one available data stream in practice.

Some methods can help reduce the channel correlation, which are shown in Fig. 2. Adjusting the angle of PDs, placing opaque boundaries in the receiver or using PDs with narrow FOV [6] can block relevant links to achieve channel decorrelation at the expense of sacrificing some receiving power. Power imbalance or power/offset allocation [5] can better utilize the spatial multiplexing, but the MIMO channel capacity is still limited due to the ill-conditioned structure of channel matrix [25]. In [7], an artificial neural network equalizer was proposed to correct the errors introduced by the ill-conditioned matrix without influencing the channel matrix directly. In recent years, using imaging receiver has been proved to be one of most efficient ways to apply MIMO in VLC system since lens can help distinguish the images of LEDs in the PD arrays [4], [8]–[12]. The analysis of imaging MIMO channel matrix can be found in [4] and [12].

On the other hand, channel modeling with multipath effects is still an open issue. Author in [5] used Rayleigh model and lognormal model to analyze the indoor optical MIMO system. In [19] and [20], authors presented indoor multipath dispersion characteristics for VLC by using recursive algorithm. An exponential decay model in [21] can also be adopted to describe multipath effects for indoor optical wireless channels.

Channel modeling, MIMO decorrelation and channel estimation/training are beyond the scope of this paper. Our work mainly focuses on designing an optical MIMO scheme with VLC-specific constraints after obtaining the channel state information, no matter whether the information is perfect or imperfect. The assumption for the MIMO channel modeling here is that the channel response in each transmission period is independent and flat, which has been widely accepted in both VLC and RF systems.

III. System Model and Problem Formulation

Considering a MIMO VLC system shown in Fig. 3, it consists of $N_t \times N_r$ optical MIMO channels with N_t LEDs in the transmitter and N_r photodetectors in the receiver. The original information bits are modulated into source data vector denoted by $\mathbf{s}(t) = [s_1(t), \cdots, s_{N_t}(t)]^T$. Without loss of generality, we ignore the time index t in the rest of the paper. Before the data vector is sent through the optical channels, it will be firstly precoded by a precoding matrix $\mathbf{F}$. We have

$$\mathbf{x} = \mathbf{F}\mathbf{s}. \tag{6}$$

Since the VLC employs IM/DD, the transmitted signal must be real-valued and unipolar (positive-valued). As a result, all vectors and matrices in this paper are real-valued, e.g., $\mathbf{s} \in \mathbb{R}^{N_t}$ and $\mathbf{F} \in \mathbb{R}^{N_t \times N_t}$. In addition, the precoded data vector $\mathbf{x} = [x_1, \cdots, x_{N_t}]^T$ cannot be transmitted directly since it may contain negative values. Thus, a DC biasing vector $\mathbf{p} = [p_1, \cdots, p_{N_t}]^T$ is added to make sure the transmitted data vector is positive.

$$\mathbf{y} = \mathbf{x} + \mathbf{p} = \mathbf{F}\mathbf{s} + \mathbf{p} \geq \mathbf{0}. \tag{7}$$

The source data s_k is assumed to be zero-mean and bounded as

$$-b_k \leq s_k \leq b_k. \tag{8}$$

A multi-level pulse amplitude modulation (PAM) could serve as a practical solution.

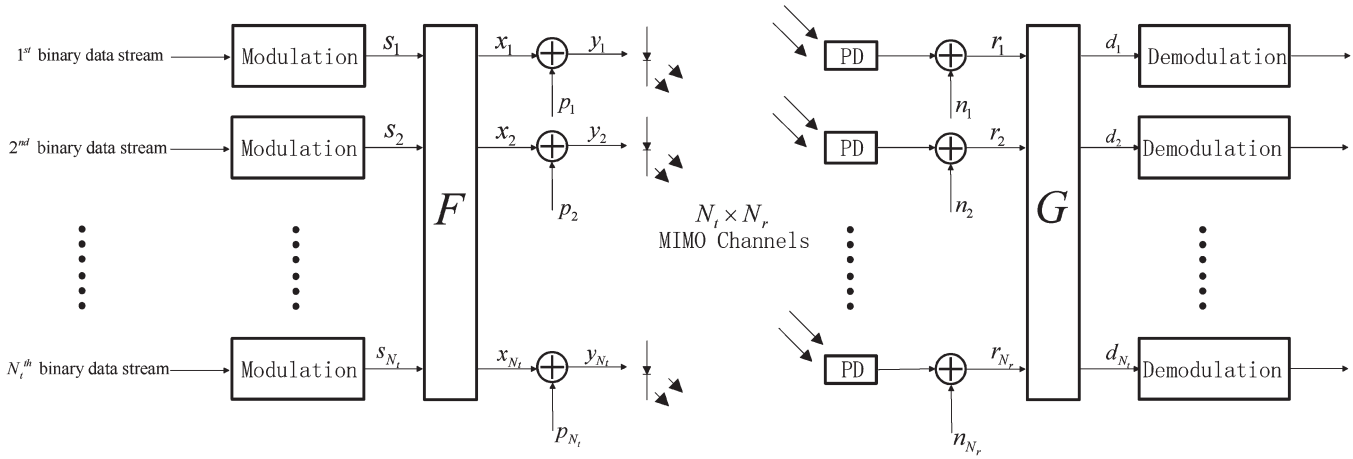

Fig. 3. Illustration of the proposed MIMO VLC system.

Since the electric signal y_i at the ith transmitter is just a linear combination of source data and DC bias p_i, and $\mathbb{E}\{s_k\} = 0$, the average optical power is

$$\mathbb{E}\{y_i\} = \sum_{k=1}^{N_t} f_{i,k}\mathbb{E}\{s_k\} + p_i = p_i \tag{9}$$

where $f_{i,k}$ denotes the element in the ith row and the jth column of the precoder matrix $\mathbf{F}$. Here, we assume that the nonlinear characteristics of LED electrical-to-optical conversion is compensated by digital pre-distortion (DPD) [17], [18] and the overall linear gain is chosen as 1 for simplicity without loss of generality.

The system can adjust the DC biasing vector $\mathbf{p}$ to achieve a specific illumination level. Thus, dimming/brightness control can be well supported in the proposed MIMO VLC system. Moreover, the transmitted signal must be positive-valued. We have

$$\mathbf{x} = \mathbf{Fs} \geq -\mathbf{p}, \tag{10}$$

or

$$x_i = \sum_{k=1}^{N_t} s_k f_{i,k} \geq -p_i. \tag{11}$$

With the constraint in (8), x_i is bounded by

$$-\sum_{k=1}^{N_t} b_k|f_{i,k}| \leq x_i \leq \sum_{k=1}^{N_t} b_k|f_{i,k}|. \tag{12}$$

Combine (11) and (12), we have

$$\sum_{k=1}^{N_t} b_k|f_{i,k}| \leq p_i, \tag{13}$$

or

$$\text{abs}(\mathbf{F})\mathbf{b} \leq \mathbf{p}. \tag{14}$$

At the receiver, PDs generate electric signal proportional to the intensity of the received optical signals. For optical MIMO system, we assume that the channel response in each transmission period is independent and flat. Then the received signal vector is

$$\mathbf{r} = \mathbf{Hy} + \mathbf{n} = \mathbf{H}(\mathbf{Fs} + \mathbf{p}) + \mathbf{n}, \tag{15}$$

where $\mathbf{H}$ denotes the $N_r \times N_t$ optical wireless MIMO channel matrix and $\mathbf{n}$ is the additive white Gaussian noise with zero mean and covariance matrix $\mathbf{R_n}$. A linear equalizer $\mathbf{G}$ is adopted to recover the transmitted data.

$$\mathbf{d} = \mathbf{Gr} = \mathbf{GHFs} + \mathbf{GHp} + \mathbf{Gn}. \tag{16}$$

After removing the bias, the data vector can be determined by MMSE detection:

$$\hat{\mathbf{s}} = \arg\min_{\mathbf{s}\in\mathbb{S}} \|\mathbf{d} - \mathbf{GHp} - \mathbf{s}\|^2 \tag{17}$$

where $\mathbb{S}$ is the set of all possible source data vectors. For PAM, after obtaining the precoder matrix $\mathbf{F}$ and the equalizer matrix $\mathbf{G}$, the decoding is $\hat{\mathbf{s}} = Q\{\mathbf{d} - \mathbf{GHp}\}$, where $Q\{\cdot\}$ is element-wise quantization according to the data alphabet.

In practical systems, before the MIMO data transmission, there are two steps. The first step is the channel estimation while the second step is the adaptive precoder and equalizer design. In this paper, the channel estimation is not included. Our work concentrates on the joint optimization of precoder and equalizer. We assume that the channel estimation can be done just as RF systems [22]. The CSI can be provided to the transmitter by another medium as the uplink, which has been accepted as a reasonable model [12], [23].

IV. Joint Precoder and Equalizer Design With Perfect Channel Information

In order to recover the information bits from the received signal, we can formulate the problem below: design the linear precoder matrix $\mathbf{F}$ at the transmitter and the linear equalizer $\mathbf{G}$ at

the receiver to minimize the mean-square error (MSE) between the transmitted data and the recovered data, i.e.,

$$\begin{aligned} \min_{\mathbf{F},\mathbf{G}} \quad & MSE(\mathbf{d},\mathbf{s},\mathbf{F},\mathbf{G}), \\ s.t. \quad & \text{abs}(\mathbf{F})\mathbf{b} \le \mathbf{p}. \end{aligned} \tag{18}$$

To begin with, we assume that the channel matrix $\mathbf{H}$ is perfectly known. We have

$$\begin{aligned} & MSE(\mathbf{d},\mathbf{s},\mathbf{F},\mathbf{G}) \\ &= \mathbb{E}\left\{\|\mathbf{d}-\mathbf{GHp}-\mathbf{s}\|^2\right\} \\ &= \mathbb{E}\left\{\left\|(\mathbf{GHF}-\mathbf{I}_{N_t})\mathbf{s}+\mathbf{Gn}\right\|^2\right\} \\ &= Tr\left((\mathbf{GHF}-\mathbf{I}_{N_t})\mathbf{R_s}(\mathbf{GHF}-\mathbf{I}_{N_t})^H\right) \\ &\quad + Tr(\mathbf{GR_nG}^H) \\ &= Tr\left(\mathbf{GHFR_s}(\mathbf{GHF})^H\right) + Tr(\mathbf{GR_nG}^H) \\ &\quad + Tr(\mathbf{R_s}) - Tr(\mathbf{GHFR_s}) - Tr\left(\mathbf{R_s}(\mathbf{GHF})^H\right) \end{aligned} \tag{19}$$

where $\mathbf{R_s} = \mathbb{E}\{\mathbf{ss}^H\}$. In this paper, the source data vector $\mathbf{s}$ and the noise vector $\mathbf{n}$ are assumed to be independent.

The corresponding optimization problem is shown in (20) at the bottom of the page. From (20), we observe that the objective function is complicated with respect to $\mathbf{F}$ and $\mathbf{G}$. A closed-form expression is not straightforward. However, an iterative algorithm can be developed. $\mathbf{F}$ and $\mathbf{G}$ are initialized with given values. Then we can update one of $\mathbf{F}$ or $\mathbf{G}$ iteratively while fixing the other.

A. Updating G Given F

Suppose at the jth iteration, $\mathbf{G}_j$ and $\mathbf{F}_j$ are obtained. At the $(j+1)$th iteration, we first update $\mathbf{G}_{j+1}$ for given $\mathbf{F}_j$. Since the constraint in (14) has nothing to do with $\mathbf{G}$, the optimal $\mathbf{G}_{j+1}$ for given $\mathbf{F}_j$ satisfies the following condition:

$$\frac{\partial MSE(\mathbf{d},\mathbf{s},\mathbf{F}_j,\mathbf{G}_{j+1})}{\partial \mathbf{G}_{j+1}} = 0. \tag{21}$$

Expanding (21), we have

$$\begin{aligned} & \frac{\partial MSE(\mathbf{d},\mathbf{s},\mathbf{F}_j,\mathbf{G}_{j+1})}{\partial \mathbf{G}_{j+1}} \\ &= 2\mathbf{G}_{j+1}\mathbf{HF}_j\mathbf{R_s}(\mathbf{HF}_j)^H + 2\mathbf{G}_{j+1}\mathbf{R_n} - 2\mathbf{R_s}(\mathbf{HF}_j)^H \\ &= 0. \end{aligned} \tag{22}$$

The optimal $\mathbf{G}$ is:

$$\mathbf{G}_{j+1} = \mathbf{R_s}(\mathbf{HF}_j)^H\left(\mathbf{HF}_j\mathbf{R_s}(\mathbf{HF}_j)^H + \mathbf{R_n}\right)^{-1}. \tag{23}$$

B. Updating F Given G

As the constraint in (14) contains the element-wise absolute operator, it is difficult to implement the traditional optimization algorithms with relaxations. On the other hand, the constraint is linear. Moreover, with the help of equations $Tr(\mathbf{AB}) = Tr(\mathbf{BA})$ and $Tr(\mathbf{X}^H\mathbf{YXW}) = \text{vec}(\mathbf{X})^H(\mathbf{W}^T \otimes \mathbf{Y})\text{vec}(\mathbf{X})$ in [24], the first term of the objective function in (20) can be rewritten as

$$\begin{aligned} & Tr(\mathbf{GHFR_s}(\mathbf{GHF})^H) \\ &= Tr(\mathbf{FR_s}\mathbf{F}^H\mathbf{H}^H\mathbf{G}^H\mathbf{GH}) \\ &= \text{vec}(\mathbf{F}^H)^H\left((\mathbf{H}^H\mathbf{G}^H\mathbf{GH}) \otimes \mathbf{R_s}\right)\text{vec}(\mathbf{F}^H). \end{aligned} \tag{24}$$

The above term turns out to be quadratic. It is easy to show that other terms in (20) are linear or constant.

The original optimization problem in (20) can be transformed into a convex linearly constrained quadratic program (LCQP) problem. Thus, we could use CVX, a software package for specifying and solving convex programs [27], to figure out the optimal $\mathbf{F}$ for given $\mathbf{G}$.

C. Convergence of Iterative Algorithm

The proposed iterative algorithm is summarized as Algorithm 1.

Algorithm 1 Iterative algorithm for joint design of $\mathbf{F}$ and $\mathbf{G}$

1: Initialization:
   1) Estimate channel matrix $\mathbf{H}$ and noise parameter $\mathbf{R_n}$.
   2) Set illumination level ($\mathbf{p}$) and modulation scheme ($\mathbf{b}$ and $\mathbf{R_s}$).
   3) Initialize precoder matrix $\mathbf{F}_0$ within constraint (14), e.g., $\mathbf{F}_0 = a\mathbf{I}_{N_t}$, where $0 < a \le \min_{i=1,\cdots,N_t}\{\frac{p_i}{b_i}\}$.
2: Iteration:
   1) Update $\mathbf{G}_j$ with given $\mathbf{F}_{j-1}$ by using (23).
   2) With $\mathbf{G}_j$, rewrite objective function (20) by (24), figure out optimal $\mathbf{F}_j$ by CVX.
   3) $j = j+1$.
3) Termination:
   1) $\|\mathbf{F}_j - \mathbf{F}_{j-1}\|^2 < \epsilon$, where ϵ is a predefined threshold;
   2) or $j = j_{max}$, where j_{max} is the predefined default max iteration number.

We can check the convergence of the iterative algorithm as follows. Given that $\mathbf{G}_j$ and $\mathbf{F}_j$ are the solutions at the jth iteration, $\mathbf{G}_{j+1}$ obtained by the closed form in (23) is the optimal solution with fixed $\mathbf{F}_j$ in the $(j+1)$th iteration. In other words, we have $MSE(\mathbf{d},\mathbf{s},\mathbf{F}_j,\mathbf{G}_{j+1}) \le MSE(\mathbf{d},\mathbf{s},\mathbf{F}_j,\mathbf{G}_j)$. Then we fix $\mathbf{G}_{j+1}$ to update $\mathbf{F}$. Since this is a convex formulation, we have $MSE(\mathbf{d},\mathbf{s},\mathbf{F}_{j+1},\mathbf{G}_{j+1}) \le MSE(\mathbf{d},\mathbf{s},\mathbf{F}_j,\mathbf{G}_{j+1})$. In the final

$$\begin{aligned} \min_{\mathbf{F},\mathbf{G}} \quad & Tr\left(\mathbf{GHFR_s}(\mathbf{GHF})^H\right) + Tr(\mathbf{GR_nG}^H) + Tr(\mathbf{R_s}) - Tr(\mathbf{GHFR_s}) - Tr\left(\mathbf{R_s}(\mathbf{GHF})^H\right) \\ s.t. \quad & \text{abs}(\mathbf{F})\mathbf{b} \le \mathbf{p} \end{aligned} \tag{20}$$

analysis, MSE is decreasing with lower bound 0 in the iterations so that the proposed algorithm will converge to a local optimum at least. Since the original optimization problem may not be joint convex with respect to both $\mathbf{G}$ and $\mathbf{F}$, the discussion of the optimality will be in our future work.

The iterative algorithm discussed in this section is called non-robust transceiver design method, because it is based on an assumption that the channel estimation is perfect. When the channel estimation contains errors, the performance of the non-robust method degrades. In the next section, we will take the channel imperfection into consideration to construct a robust precoder/equalizer design method.

V. Joint Precoder and Equalizer Design With Imperfect Channel Information

In most cases, the channel state information is not perfectly available. In this part, we assume that the MIMO VLC system has the estimated CSI. The channel estimation errors are taken into account, we have

$$\mathbf{H} = \hat{\mathbf{H}} + \Delta\mathbf{H}, \tag{25}$$

where $\hat{\mathbf{H}}$ is the estimated CSI, while $\Delta\mathbf{H}$ is the corresponding channel estimation error whose elements are Gaussian random variables with zero mean. It is natural to formulate the estimation errors as Gaussian model [5]. In general, the $N_r \times N_t$ matrix $\Delta\mathbf{H}$ can be written as

$$\Delta\mathbf{H} = \mathbf{\Sigma}^{1/2}\mathbf{H}_W\mathbf{\Psi}^{1/2}, \tag{26}$$

where the elements of the $N_r \times N_t$ matrix $\mathbf{H}_W$ are independent and identically distributed (i.i.d.) Gaussian random variables with zero mean and unit variance [26]. The $N_r \times N_r$ matrix $\mathbf{\Sigma}$ and $N_t \times N_t$ matrix $\mathbf{\Psi}$ are the row and column covariance matrices of $\Delta\mathbf{H}$, respectively [26].

Then the MSE function can be similarly derived as

$$\begin{aligned}
&MSE(\mathbf{d},\mathbf{s},\mathbf{F},\mathbf{G})\\
&\quad= \mathbb{E}\left\{\|\mathbf{d}-\mathbf{G}\hat{\mathbf{H}}\mathbf{p}-\mathbf{s}\|^2\right\}\\
&\quad= \mathbb{E}\left\{\|\mathbf{GHFs}+\mathbf{GHp}+\mathbf{Gn}-\mathbf{G}\hat{\mathbf{H}}\mathbf{p}-\mathbf{s}\|^2\right\}\\
&\quad= \mathbb{E}\left\{\left\|(\mathbf{GHF}-\mathbf{I}_{N_t})\mathbf{s}+\mathbf{G}\Delta\mathbf{Hp}+\mathbf{Gn}\right\|^2\right\}\\
&\quad= \mathbb{E}_{\Delta\mathbf{H}}\left\{Tr\left((\mathbf{GHF}-\mathbf{I}_{N_t})\mathbf{R_s}(\mathbf{GHF}-\mathbf{I}_{N_t})^H\right)\right\}\\
&\qquad+\mathbb{E}_{\Delta\mathbf{H}}\left\{Tr(\mathbf{G}\Delta\mathbf{Hp}(\mathbf{G}\Delta\mathbf{Hp})^H)\right\}+Tr(\mathbf{GR_nG}^H)\\
&\quad= \mathbb{E}_{\Delta\mathbf{H}}\left\{Tr(\mathbf{GHFR_s}(\mathbf{GHF})^H)\right\}+Tr(\mathbf{R_s})\\
&\qquad+\mathbb{E}_{\Delta\mathbf{H}}\left\{Tr(\mathbf{G}\Delta\mathbf{Hp}(\mathbf{G}\Delta\mathbf{Hp})^H)\right\}+Tr(\mathbf{GR_nG}^H)\\
&\qquad-Tr(\mathbf{G}\hat{\mathbf{H}}\mathbf{FR_s})-Tr\left(\mathbf{R_s}(\mathbf{G}\hat{\mathbf{H}}\mathbf{F})^H\right).
\end{aligned} \tag{27}$$

For the first term above, we have

$$\mathbb{E}_{\Delta\mathbf{H}}\left\{Tr(\mathbf{GHFR_s}(\mathbf{GHF})^H)\right\} = Tr(\mathbf{G}\mathbb{E}_{\Delta\mathbf{H}}\left\{\mathbf{HFR_sF}^H\mathbf{H}^H\right\}\mathbf{G}^H), \tag{28}$$

and

$$\begin{aligned}
&\mathbb{E}_{\Delta\mathbf{H}}\left\{\mathbf{HFR_sF}^H\mathbf{H}^H\right\}\\
&\quad= \mathbb{E}_{\Delta\mathbf{H}}\left\{(\hat{\mathbf{H}}+\Delta\mathbf{H})\mathbf{FR_sF}^H(\hat{\mathbf{H}}+\Delta\mathbf{H})^H\right\}\\
&\quad= Tr(\mathbf{FR_sF}^H\mathbf{\Psi})\mathbf{\Sigma}+\hat{\mathbf{H}}\mathbf{FR_sF}^H\hat{\mathbf{H}}^H.
\end{aligned} \tag{29}$$

For the third term in (27), we have

$$\begin{aligned}
&\mathbb{E}_{\Delta\mathbf{H}}\left\{Tr(\mathbf{G}\Delta\mathbf{Hp}(\mathbf{G}\Delta\mathbf{Hp})^H)\right\}\\
&\quad= Tr\left(\mathbf{G}\mathbb{E}_{\Delta\mathbf{H}}\left\{\Delta\mathbf{Hpp}^H\Delta\mathbf{H}^H\right\}\mathbf{G}^H\right)\\
&\quad= Tr(\mathbf{G}Tr(\mathbf{pp}^H\mathbf{\Psi})\mathbf{\Sigma}\mathbf{G}^H).
\end{aligned} \tag{30}$$

Combing (26)$\sim$(28), (25) can be reduced to (31), shown at the bottom of the page. For (31), similarly, we can also develop an iterative algorithm.

A. Updating G Given F

The derivative to (31) can be rewritten as

$$\begin{aligned}
&\frac{\partial MSE(\mathbf{d},\mathbf{s},\mathbf{F}_j,\mathbf{G}_{j+1})}{\partial\mathbf{G}_{j+1}}\\
&\quad= 2\mathbf{G}_{j+1}\left(Tr(\mathbf{F}_j\mathbf{R_s}\mathbf{F}_j^H\mathbf{\Psi})\mathbf{\Sigma}+\hat{\mathbf{H}}\mathbf{F}_j\mathbf{R_s}\mathbf{F}_j^H\hat{\mathbf{H}}^H\right)\\
&\qquad+2\mathbf{G}_{j+1}Tr(\mathbf{pp}^H\mathbf{\Psi})\mathbf{\Sigma}+2\mathbf{G}_{j+1}\mathbf{R_n}-2\mathbf{R_s}(\hat{\mathbf{H}}\mathbf{F}_j)^H.
\end{aligned} \tag{32}$$

The optimal solution of (31) with given $\mathbf{F}$ is achieved when $\partial MSE(\mathbf{d},\mathbf{s},\mathbf{F}_j,\mathbf{G}_{j+1})/\partial\mathbf{G}_{j+1}=0$. The closed-form expression for optimal $\mathbf{G}$ with given $\mathbf{F}$ is

$$\begin{aligned}
\mathbf{G}_{j+1} = \mathbf{R_s}(\hat{\mathbf{H}}\mathbf{F}_j)^H\Bigg(&Tr(\mathbf{F}_j\mathbf{R_s}\mathbf{F}_j^H\mathbf{\Psi})\mathbf{\Sigma}+\hat{\mathbf{H}}\mathbf{F}_j\mathbf{R_s}\mathbf{F}_j^H\hat{\mathbf{H}}^H\\
&+Tr(\mathbf{pp}^H\mathbf{\Psi})\mathbf{\Sigma}+\mathbf{R_n}\Bigg)^{-1}.
\end{aligned} \tag{33}$$

B. Updating F Given G

Given $\mathbf{G}$, the original optimization problem can also be transformed into the convex LCQP problem. The first term in (31) can be rewritten as:

$$\begin{aligned}
&Tr\left(\mathbf{G}\left(Tr(\mathbf{FR_sF}^H\mathbf{\Psi})\mathbf{\Sigma}+\hat{\mathbf{H}}\mathbf{FR_sF}^H\hat{\mathbf{H}}^H\right)\mathbf{G}^H\right)\\
&\quad= Tr\left(\mathbf{G}Tr(\mathbf{FR_sF}^H\mathbf{\Psi})\mathbf{\Sigma}\mathbf{G}^H\right)+Tr(\mathbf{G}\hat{\mathbf{H}}\mathbf{FR_sF}^H\hat{\mathbf{H}}^H\mathbf{G}^H)\\
&\quad= Tr(\mathbf{FR_sF}^H\mathbf{\Psi})Tr(\mathbf{G}\mathbf{\Sigma}\mathbf{G}^H)+Tr(\mathbf{G}\hat{\mathbf{H}}\mathbf{FR_sF}^H\hat{\mathbf{H}}^H\mathbf{G}^H)\\
&\quad= \mathrm{vec}(\mathbf{F}^H)^H(\mathbf{\Psi}^H\otimes\mathbf{R_s})\mathrm{vec}(\mathbf{F}^H)Tr(\mathbf{G}\mathbf{\Sigma}\mathbf{G}^H)\\
&\qquad+\mathrm{vec}(\mathbf{F}^H)^H\left((\hat{\mathbf{H}}^H\mathbf{G}^H\mathbf{G}\hat{\mathbf{H}})\otimes\mathbf{R_s}\right)\mathrm{vec}(\mathbf{F}^H).
\end{aligned} \tag{34}$$

$$\begin{aligned}
\min_{\mathbf{F},\mathbf{G}}\quad &Tr\left(\mathbf{G}\left(Tr(\mathbf{FR_sF}^H\mathbf{\Psi})\mathbf{\Sigma}+\hat{\mathbf{H}}\mathbf{FR_sF}^H\hat{\mathbf{H}}^H\right)\mathbf{G}^H\right)+Tr\left(\mathbf{G}Tr(\mathbf{pp}^H\mathbf{\Psi})\mathbf{\Sigma}\mathbf{G}^H\right)+Tr(\mathbf{R_s})\\
&+Tr(\mathbf{GR_nG}^H)-Tr(\mathbf{G}\hat{\mathbf{H}}\mathbf{FR_s})-Tr\left(\mathbf{R_s}(\mathbf{G}\hat{\mathbf{H}}\mathbf{F})^H\right)\\
s.t.\quad &\mathrm{abs}(\mathbf{F})\mathbf{b}\le\mathbf{p}
\end{aligned} \tag{31}$$

Similarly, with the help of CVX, the optimal $\mathbf{F}$ for given $\mathbf{G}$ can be obtained numerically.

The details of the iterative algorithm and convergence analysis are just the same as the discussion shown in previous section.

VI. Numerical Results and Discussions

In previous sections, we have performed theoretical analysis of the optimization for the MIMO VLC system. The optimal solution can be easily implemented into the practical design of the precoder and equalizer. In this section, we would like to illustrate some simulation results to verify the proposed MIMO VLC system and the minimum MSE (MMSE) iterative algorithm.

Without loss of generality, according to the MIMO channel model used in [5] we generate and then fix the estimated channel matrix. Set the example as:

$$\hat{\mathbf{H}} = \begin{bmatrix} 1.3060 & 0.1122 & 0.6696 & 1.4911 \\ 1.0030 & 0.7189 & 0.7195 & 0.0920 \\ 0.8754 & 0.9745 & 0.2235 & 0.6634 \\ 0.5553 & 0.3450 & 1.0194 & 1.6516 \end{bmatrix} \tag{35}$$

For the ideal case, the actual channel matrix equals the estimated one perfectly. However, for the realistic case, there are estimation errors, which is discussed in Section IV. Moreover, the corresponding covariance matrices are chosen as

$$\mathbf{\Psi} = \begin{bmatrix} 1 & \alpha & \alpha^2 & \alpha^3 \\ \alpha & 1 & \alpha & \alpha^2 \\ \alpha^2 & \alpha & 1 & \alpha \\ \alpha^3 & \alpha^2 & \alpha & 1 \end{bmatrix}, \tag{36}$$

$$\mathbf{\Sigma} = \sigma_e^2 \begin{bmatrix} 1 & \beta & \beta^2 & \beta^3 \\ \beta & 1 & \beta & \beta^2 \\ \beta^2 & \beta & 1 & \beta \\ \beta^3 & \beta^2 & \beta & 1 \end{bmatrix}, \tag{37}$$

which are also adopted in [26]. In (37), σ_e^2 represents the variance of channel imperfection. In each channel realization, the channel estimation error matrix can be generated by (26).

Additionally, in our simulation, 2-PAM is applied. Both the signals and the noises are assumed to be i.i.d., which is also reasonable in practical systems. Thus, $\mathbf{R_s} = \sigma_s^2 \mathbf{I}_4$ and $\mathbf{R_n} = \sigma_n^2 \mathbf{I}_4$, where $\mathbf{I}_4$ is the identity matrix of dimension 4, σ_s^2 is the variance of the input signal or so called input signal power and σ_n^2 is the variance of the noise, namely, noise power.

To begin with, we demonstrate the convergence performance of the iterative algorithms. Fig. 4 illustrates an example with DC biasing vector set as $\mathbf{p} = [9, 9, 9, 9]^T$ and both the input signal power and the noise power set to be 1. For the robust case, the channel imperfection is presented by $\alpha = 0.6$, $\beta = 0.5$ and $\sigma_e^2 = 0.002$. It can be seen that the iterative algorithms converge to the optimal solutions after about 20 iterations with the initial $\mathbf{F}$ set as $\mathbf{I}_4$. Actually, the channel of the indoor VLC system can be treated as pseudo static. The channel matrix does not change frequently. Off-line processing is acceptable. In practice, the optimization algorithm can be done at the transmitter to reduce the complexity of the receiver. After obtaining the optimal precoder matrix and equalizer matrix, the equalizer matrix can be provided to the receiver as side information through other reliable link. The obtained precoder matrix and equalizer matrix are valid for a reasonably long period since the VLC scenario is static in most cases.

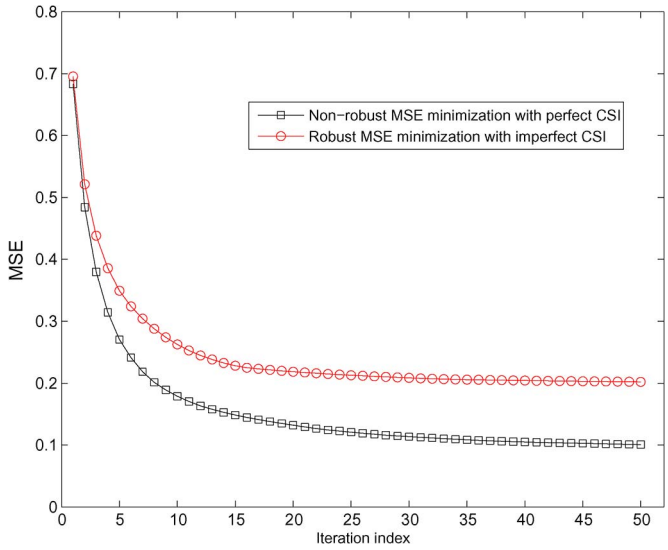

Fig. 4. Convergence performance of the iterative algorithms with $\alpha = 0.6$, $\beta = 0.5$ and $\sigma_e^2 = 0.002$ (for robust case).

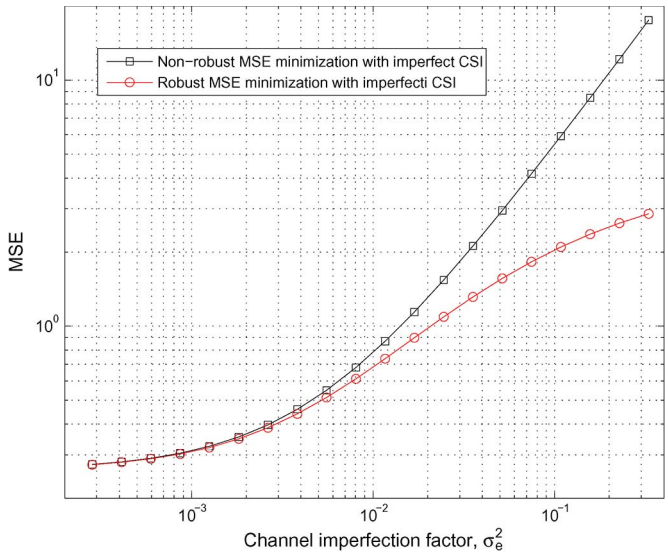

Fig. 5. Impact of the channel imperfection and the robustness of the proposed iterative algorithm ($\mathbf{p} = [5, 5, 5, 5]^T$).

In the following, the robustness of our proposed iterative algorithm by taking into account the channel imperfection is analyzed. The signal power and the noise power are set the same as in Fig. 4. The MSE performance is simulated with different variances of the channel imperfection. In [5], authors have shown that the performance is sensitive to the high CSI imperfection. In our results shown in Fig. 5, we can draw the same conclusion that the MSE becomes worse and worse with the increase of the channel imperfection factor. However, the proposed robust MSE minimization scheme performs better than the one that does not consider channel uncertainties. Since we take the channel estimation error into account for the joint optimization of precoder and equalizer design, our algorithm

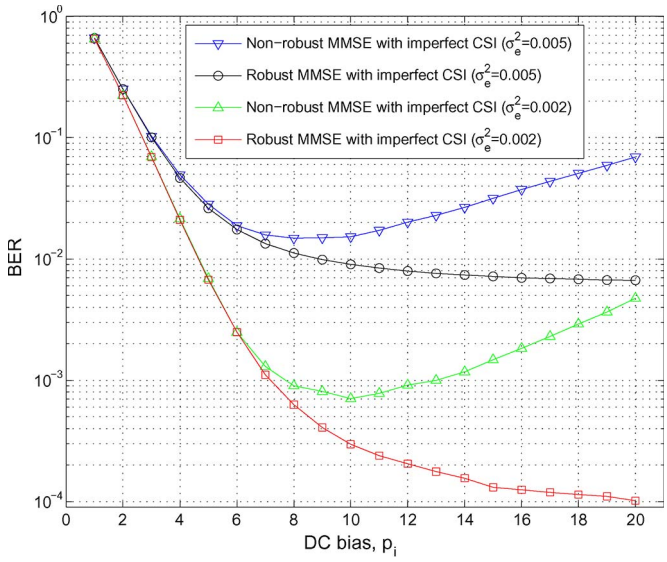

Fig. 6. BER performance of the proposed iterative algorithm.

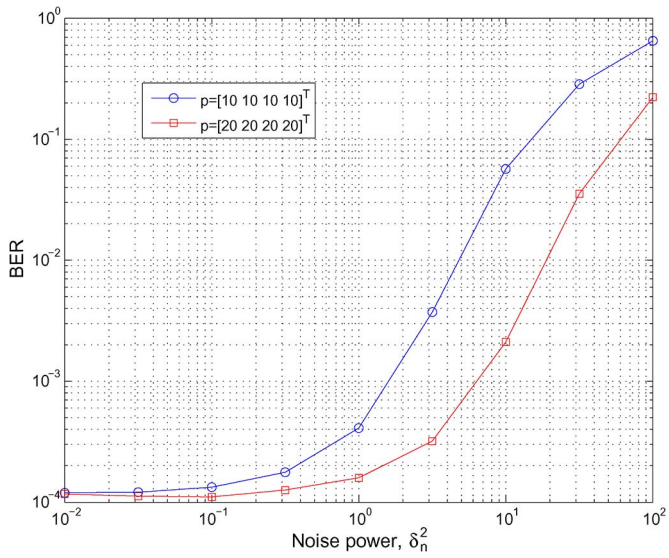

Fig. 7. BER performance of the proposed robust scheme with various noise power.

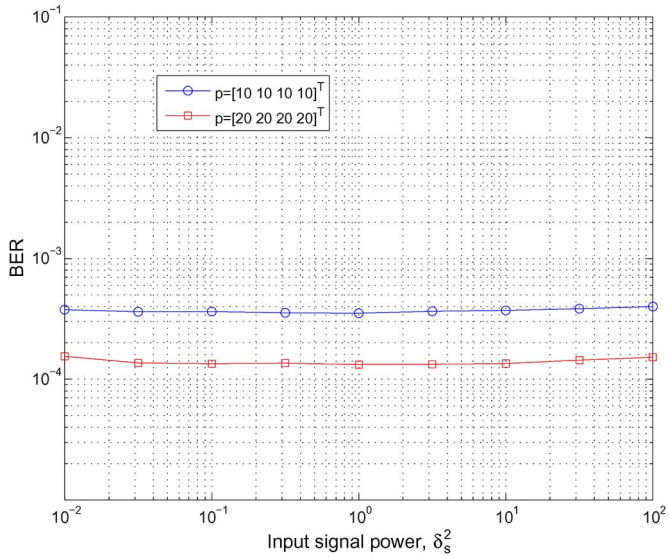

Fig. 8. BER performance of the proposed robust scheme with various input signal power.

has the potential to improve the performance against the severe impact of the CSI imperfection.

Next, we simulate the bit error rate (BER) performance. We still fix the noise power and the signal power to be 1, and then adjust the DC bias p_i so that the dimming support of the proposed system can be also demonstrated. Each BER is calculated after 10^7 times channel realizations. From Fig. 6, it is seen that the BER cannot meet the forward error correction limit (10^{-3}) when both the channel imperfection ($\alpha = 0.6$, $\beta = 0.5$ and $\sigma_e^2 = 0.005$) and the noise power ($\sigma_n^2 = 1$) are significant. Even for the case that is not so bad ($\sigma_e^2 = 0.002$), it is still difficult for the non-robust scheme to meet the forward error correction limit. On the other hand, the robust MMSE algorithm performs much better and can enhance the BER performance to an acceptable level. Moreover, the BER of the robust scheme decreases significantly with the DC bias increasing. The explanation can be intuitive. When the DC bias becomes large, considering the constraint abs($\mathbf{F}$)$\mathbf{b} \leq \mathbf{p}$ in the optimization problem (18), the feasible set of precoder matrix enlarges and a broader dynamic range of the LED transmitter can be utilized. Thus, a better solution can be achieved with an enlarged feasible set. In other words, the optimal precoder obtained by our robust scheme guarantees a properly higher transmitted signal power level with a broadened operation range of the LED transmitter. On the contrary, without considering the imperfect CSI, BER performance becomes worse when DC bias is large, since the channel imperfection influences the accuracy of the DC bias estimation thus degrades the performance in the data recovery. In other words, the DC bias estimation error $\mathbf{G}\Delta\mathbf{H}\mathbf{p}$ increases when DC bias $\mathbf{p}$ becomes larger and larger. From Fig. 6, we observe that the DC bias estimation error dominates the BER degradation in the non-robust scheme when the DC level is larger than 10.

To better understand the performance of our proposed MIMO VLC system and the robust MMSE scheme. We also simulate the BER with various noise power and input signal power. First, we fix the input signal power as $\sigma_s^2 = 1$ and change the noise power. The channel imperfection is denoted by $\alpha = 0.6$, $\beta = 0.5$ and $\sigma_e^2 = 0.002$. The simulation result is shown in Fig. 7. Intuitively, the BER will decrease with the reduction of the noise power. Moreover, we see that the BER performance degradation is dominated by the channel estimation error when the noise is lowered to a level. That is also the motivation why we should take into account the channel uncertainties into the transceiver design.

Second, we fix the noise power to be 1 and change the input signal power σ_s^2. The channel imperfection is denoted by $\alpha = 0.6$, $\beta = 0.5$ and $\sigma_e^2 = 0.002$. The simulation result is shown in Fig. 8. It is interesting to be seen that the BER remains the same level with the various input signal power. The reason is that the precoder can be adaptively optimized in our proposed MIMO scheme, so that the precoded transmitted signals can obtain the similar and properly high power level with the same illumination constraint.

In the final analysis, our proposed MIMO scheme by considering channel uncertainties is robust to combat the influence caused by the channel estimation imperfection. In addition, the transceiver can be adaptively optimized according to various input signals and different illumination levels.

VII. Conclusion

The MIMO VLC system has the potential to enhance the indoor optical wireless communication. This paper studies the joint optimization for the precoder and equalizer design in a proposed MIMO VLC system. The first contribution of this paper is that the proposed system can effectively support the lighting requirements such as flickering/dimming control, which is suitable for the practical utilization. Moreover, besides the transceiver design with perfect CSI, we also take into account channel uncertainties for joint optimization in the MIMO VLC system. Iterative MSE minimization algorithms are developed for both the non-robust and robust transceiver design. Simulation results validate the effectiveness of our proposed scheme against the channel estimation imperfection. By taking into account the channel estimation errors, the proposed joint optimization method demonstrates the BER improvements in the scenario of imperfect channel estimation.

References

[1] H. Elgala, R. Mesleh, and H. Haas, "Indoor optical wireless communication: Potential and state-of-the-art," *IEEE Commun. Mag.*, vol. 49, no. 9, pp. 56–62, Dec. 2011.

[2] *IEEE Standard for Local and Metropolitan Area Networks—Part 15.7: Short-Range Wireless Optical Communication Using Visible Light*, IEEE Std 802.15.7, Sep. 2011.

[3] R. Mesleh, R. Mehmood, H. Elgala, and H. Haas, "Indoor MIMO optical wireless communication using spatial modulation," in *Proc. IEEE ICC*, May 2010, pp. 1–5.

[4] L. Zeng, *et al.*, "High data rate multiple input multple output (MIMO) optical wireless communications using white LED lighting," *IEEE J. Sel. Areas Commmun.*, vol. 27, no. 9, pp. 1654–1662, Dec. 2009.

[5] K. H. Park, Y. C. Ko, and M. S. Alouini, "On the power and offset allocation for rate adaptation of spatial multiplexing in optical wireless MIMO channels," *IEEE Trans. Commmun.*, vol. 61, no. 4, pp. 1535–1543, Apr. 2013.

[6] T. Fath and H. Haas, "Performance comparison of MIMO techniques for optical wireless communications in indoor environments," *IEEE Trans. Commmun.*, vol. 61, no. 2, pp. 733–742, Feb. 2013.

[7] P. A. Haigh, Z. Ghassemlooy, I. Papakonstantinou, and F. Tedde, "A MIMO-ANN system for increasing data rates in organic visible light communications systems," in *Proc. IEEE ICC*, Jun. 2010, pp. 5322–5327.

[8] K. D. Dambul, D. C. O'Brien, and G. Faulkner, "Indoor optical wireless MIMO system with an imaging receiver," *IEEE Photon. Technol. Lett.*, vol. 23, no. 2, pp. 97–99, Jan. 2011.

[9] T. Q. Wang, Y. A. Sekercioglu, and J. Armstrong, "Hemispherical lens based imaging receiver for MIMO optical wireless communications," in *Proc. IEEE Globecom Workshop OWC*, Dec. 2012, pp. 1239–1243.

[10] A. H. Azhar, T.-A. Tran, and D. O'Brien, "Demonstration of high-speed data transmission using MIMO-OFDM visible light communications," in *Proc. IEEE Globecom Workshop OWC*, Dec. 2010, pp. 1052–1056.

[11] A. H. Azhar, T.-A. Tran, and D. C. O'Brien, "A gigabit/s indoor wireless transmission using MIMO-OFDM visible-light communications," *IEEE Photon. Technol. Lett.*, vol. 25, no. 2, pp. 171–174, Jan. 2013.

[12] P. M. Butala, H. Elgala, and T. D. C. Little, "SVD-VLC: A novel capacity maximizing VLC MIMO system architecture under illumination constraints," in *Proc. IEEE Globecom Workshop OWC*, Dec. 2013, pp. 1087–1092.

[13] A. Burton, H. L. Minh, Z. Ghassemlooy, E. Bentley, and C. Botella, "Experimental demonstration of 50-Mb/s visible light communications using 4 × 4 MIMO," *IEEE Photon. Technol. Lett.*, vol. 26, no. 9, pp. 945–948, May 2014.

[14] M. Biagi and A. M. Vegni, "Enabling high data rate VLC via MIMO-LEDs PPM," in *Proc. IEEE Globecom Workshop OWC*, Dec. 2013, pp. 1058–1063.

[15] F. R. Gfeller and U. H. Bapst, "Wireless in-house data communication via diffuse infrared radiation," *Proc. IEEE*, vol. 67, pp. 1474–1486, Nov. 1979.

[16] J. M. Kahn and J. R. Barry, "Wireless Infrared Communications," *Proc. IEEE*, vol. 85, no. 2, pp. 265–298, Feb. 1997.

[17] H. Elgala, R. Mesleh, and H. Haas, "Non-linearity effects and predistortion in optical OFDM wireless transmission using LEDs," *Int. J. Ultra Wideband Commun. Syst.*, vol. 1, no. 2, pp. 143–150, Nov. 2009.

[18] G. Stepniak, J. Siuzdak, and P. Zwierko, "Compensation of a VLC phosphorescent white LED nonlinearity by means of volterra DFE," *IEEE Photon. Technol. Lett.*, vol. 25, no. 16, pp. 1597–1600, Aug. 2010.

[19] J. R. Barry, J. M. Kahn, W. J. Krause, E. A. Lee, and D. G. Messerschmitt, "Simulation of multipath impulse response for indoor wireless optical channels," *IEEE J. Sel. Areas Commmun.*, vol. 11, no. 3, pp. 367–379, Apr. 1993.

[20] K. Lee, H. Park, and J. R. Barry, "Indoor channel characteristics for visible light communications," *IEEE Commun. Lett.*, vol. 15, no. 2, pp. 217–219, Feb. 2011.

[21] V. Jungnickel, V. Pohl, S. Nonnig, and C. von Helmolt, "A physical model of the wireless infrared communication channel," *IEEE J. Sel. Areas Commmun.*, vol. 20, no. 3, pp. 631–640, Apr. 2002.

[22] X. Dai, W. Zhang, J. Xu, J. E. Mitchell, and Y. Yang, "Kalman interpolation filter for channel estimation of LTE downlink in high-mobility environments," *EURASIP J. Wireless Commun. Netw.*, vol. 2012, no. 232, pp. 1–14, Jul. 2012.

[23] M. B. Rahaim, A. M. Vegni, and T. D. C. Little, "A hybrid radio frequency and broadcast visible light communication system," in *Proc. IEEE Globecom Workshop OWC*, Dec. 2011, pp. 792–796.

[24] R. Horn and C. Johnson, *Topics in Matrix Analysis*. New York, NY, USA: Cambridge Univ. Press, 1991.

[25] D. Tse and P. Viswanath, *Fundamentals of Wireless Communication*. New York, NY, USA: Cambridge Univ. Press, 2005.

[26] C. Xing, S. Ma, and Y. C. Wu, "Robust joint design of linear relay precoder and destination equalizer for dual-hop amplify-and-forward MIMO relay systems," *IEEE Trans. Signal Process.*, vol. 58, no. 4, pp. 2273–2283, Apr. 2010.

[27] CVX Research, Inc., "CVX: Matlab software for disciplined convex programming, version 2.0 (beta)," Jun. 2013.

[28] Z. Yu, R. J. Baxley, and G. T. Zhou, "EVM and achievable data rate analysis of clipped OFDM signals in visible light communication," *EURASIP J. Wireless Commun. Netw.*, vol. 2012, no. 321, pp. 1–16, Oct. 2012.

Kai Ying (S'14) received the B.S. degree and the M.E. degree from the Department of Electronic Engineering, Shanghai Jiao Tong University, Shanghai, China, in 2010 and 2013, respectively, and the M.S. degree from the School of Electrical and Computer Engineering, Georgia Institute of Technology, Atlanta, GA, in 2013. Currently, he is working toward the Ph.D. degree at Georgia Institute of Technology. His research interests include nonlinear signal processing and optical wireless communications.

Hua Qian (S'01–M'05–SM'13) received the B.S. and M.S. degrees from Department of Electrical Engineering, Tsinghua University in 1998 and 2000, respectively, and the Ph.D. degree from the School of Electrical and Computer Engineering, Georgia Institute of Technology in 2005. He is currently a Full Professor with the Shanghai Research Center for Wireless Communications, Shanghai Institute of Microsystem and Information Technology Research Institute, Chinese Academy of Sciences. He also serves as an Adjunct Professor with ShanghaiTech University. His current research interests include nonlinear signal processing and system design of wireless communications.

Robert J. Baxley (S'04–M'08–SM'13) received the B.S., M.S., and Ph.D. degrees in electrical engineering from Georgia Tech. In the course of his graduate work, he was the recipient of the Sigma Xi Award, the National Science Foundation Graduate Research Fellowship Program award, the Grand Prize in the SAIC student paper competition, and the Georgia Tech Center for Signal & Image Processing Outstanding Research Award. From 2008 to 2014, he was employed at the Georgia Tech Research Institute (GTRI) where he served as the Director of the Software Defined Radio Laboratory among other roles. While at GTRI, he led the GTRI team that placed second out of 90 teams in the DARPA Spectrum Challenge. He is currently the Chief Engineer at Bastille. He also holds an Adjunct Faculty appointment in the Georgia Tech School of Electrical and Computer Engineering. His research interests are in the areas of cognitive radio, wireless security, and signal processing for communications systems. From 2012 to 2014, he served as an Associate Editor for *Digital Signal Processing*. He is a member of the Association of Old Crows.

Saijie Yao received the B.S. degree from Nanjing University and is currently pursuing the Ph.D. degree at the Shanghai Institute of Microsystem and Information Technology, Chinese Academy of Sciences. His research interests include nonlinear signal processing and adaptive beamforming.